

Effect of surface relaxation of rhodochrosite (104) and substitution of Mn by Ca on the electronic structure of rhodochrosite

Jingqi Zhang¹, Qin Zhang^{2,3,4}, Tiebin Zhang¹

¹ Mining College, Guizhou University, Guiyang 550025, China

² Guizhou Academy of Sciences, 550001

³ National & Local Joint Laboratory of Engineering for Effective Utilization of Regional Mineral Resources from Karst Areas, Guiyang 550025, China

⁴ Guizhou Key Lab of Comprehensive Utilization of Nonmetallic Mineral Resources, Guiyang 550025, China

Corresponding author: zq6736@163.com(Qin Zhang)

Abstract: To explore the difference between the surface and crystal structure of rhodochrosite, relaxation and reconstruction of the rhodochrosite (104) surface are studied by using Density Functional Theory. The calculation results indicated that the C and O atoms with lower reactivity tend to be enriched on the surface, while the Mn atoms with the highest reactivity moved away from the surface. The band gap width decreased from 1.814 eV to 1.614 eV after the formation of the rhodochrosite (104) surface. The electrons on the rhodochrosite (104) surface are more active than crystal. Ca substitution makes the atomic activity on the (104) surface of rhodochrosite more stable. Ca substitution reduces the ability of the surface of rhodochrosite to absorb external electrons, and the surface electrical properties decrease.

Keywords: density functional theory, rhodochrosite, surface relaxation, surface electrical property

1. Introduction

More than 90% of manganese ore resources in China belong to low-grade poor manganese ore with complex composition and finely disseminated grain (Zhou et al., 2015). Manganese metal and its minerals are widely used in the aluminum industry, steel industry, etc (Zhang et al., 2007). Due to its importance in the metallurgical industry, manganese is considered to be one of national strategic resources (Kirchmeyer et al., 2005; Zhang and Cheng 2007). To meet the country's demand for metallic manganese, it is of great practical significance to develop low-grade rhodochrosite products. The flotation is one of the most effective methods to increase the recovery of fine-grained low-grade rhodochrosite (Luo et al., 2018; Rahimi et al., 2017). The flotation efficiency is determined by the surface properties of the minerals. The study of the surface properties of minerals is an effective method for understanding the principle of rhodochrosite flotation. The surface properties of minerals are closely relevant to the crystal structure. The form of the surface formed will greatly affect the properties of the mineral surface. There is a significant difference in the surface formed by the substitution of impurity atoms. Impurity atoms will change the electronic structure of the mineral surface. The surface formed by mineral crystals after the substitution of impurity atoms is very different from the surface formed by minerals not substituted by impurity atoms.

The surface structure formed has a certain relationship with the internal structure of the crystal. When building a cleaved surface in Materials Studio software, an ideal surface was formed. In the actual process, the ideal surface relaxes and restructures, and the spatial positions of the atoms change such that the surface energy is the lowest. A surface structure that differs from the ideal surface is formed. This results in a significant difference between the actual surface and the ideal surface.

The ideal zinc blende (100) surface calculated by Density Functional Theory is used to analyze relaxation and reconstruction, and the experiment is carried out by low energy electron diffraction (LEED). The results show that the calculated results are in good agreement with the experimental

value (Chen et al., 2020). Used DEPES to compare the surface relaxation of Pt(111) and Cu/Pt(111) with the surface relaxation calculated by Density Functional Theory, and concluded that the DEPES test results are consistent with the Density Functional Theory calculation results (Morawski et al., 2016). It shows that it is feasible to analyze the relaxation and reconstruction of mineral surface by Density Functional Theory calculation.

Density Functional Theory was used to study the influence of the surface relaxation of chalcopyrite on the surface properties. It was found that relaxation and reconstruction occurred after the chalcopyrite formed the surface. The metal atoms of chalcopyrite moved away from the surface, and the S atoms tend to move towards the surface (Sarvaramini et al., 2017). Research about the surface of maghemite (001) found that O atoms moved to the surface after relaxation (Bentarcourt et al., 2018). The phenomenon of surface relaxation and reconstruction of chalcopyrite makes chalcopyrite surface form disulfides, metal sulfides and metal bonds (Oliveira et al., 2010). Studies based on Density Functional Theory show that surface relaxation and reconstruction increase the bond length of CuS and FeS. The sulfur-rich surface and irregular atom aggregation caused by surface relaxation and reconstruction greatly affect the flotation effective of chalcopyrite (Wen et al., 2013). Through studying the influence of Fe, Mn and Cd impurities in sphalerite on the electronic structure, it is found that Fe 3d and Mn 3d orbitals appear in the band gap. The impurity energy level is conducive to the transfer of electrons from the valence band to the conduction band, which improves surface conductivity and electrochemical activity (Chen et al., 2010). Density Functional Theory calculations show that the spodumene impurity substituted surface is more conducive to the adsorption of oleic acid than the unsubstituted surface (Zhu et al., 2020).

The Mn element in rhodochrosite is often replaced by other impurity atoms. The substitution of Mn by this impurity element affects the flotation effective of rhodochrosite (He et al., 2020). In this paper, Density Functional Theory is used to study the surface relaxation and reconstruction of rhodochrosite crystal after forming the (104) surface, and the influence of Ca atom substitution on the electronic structure of the rhodochrosite (104) surface. The Band Structure, Density of States and surface electrical properties are used to compare and analyze the surface properties before and after Ca substitution. Surface relaxation and reconstruction are important factors in the process of surface research. Surface relaxation and reconstruction make the properties of the surface greatly change. Based on surface relaxation and reconstruction, research the influence of impurity atom substitution on the surface properties of rhodochrosite. This is of great significance for understanding the flotation mechanism of rhodochrosite, and can explain the flotation principle of rhodochrosite to a certain extent.

2. Theoretical models and methodology

In this paper, the Density Functional Theory calculation is performed by CASTEP module (Milman et al., 2010) of Materials Studio software. The rhodochrosite crystal model (Graf 1961) was shown in Fig. 1, and the cell parameters are $a=b=4.7771 \text{ \AA}$, $c=15.6640 \text{ \AA}$, $\alpha=\beta=90^\circ$, $\gamma=120^\circ$. The crystal geometry optimization process of rhodochrosite includes three aspects, which are exchange-correlation functional (Yanai et al., 2004), the plane wave cut-off energy for the ultra-soft pseudo-potential (Parker et al., 2006), and K point in Brillouin zone (Monkhorst et al., 1976). Broyden-Fletcher-Goldfarb-Shanno (BFGS) (Pfrommer et al., 1997) algorithm was used to optimize the crystal structure. The interaction between electron and ion nucleus is described by ultra-soft pseudopotential (Vanderbilt et al., 1990). The geometric optimization is set according to the following convergence accuracy. The convergence accuracy of maximum force is set to 0.1 eV/Å, maximum stress is set to 0.2 GPa and maximum displacement is set to 0.005 Å. The total energy is set to 5.0e-5 eV/atom and the convergence precision of SCF is set to 2.0e-6 eV/atom respectively. All atomic orbitals involved in the calculation are $C2s^22p^2$, $O2s^22p^4$, $Mn3d^54s^2$ and $Ca3s^23p^64s^2$.

Through the conditional test of the cut-off energy, the K point in Brillouin zone, and the exchange correlation function. The final selection of the cut-off energy was 440eV, the Brillouin zone was sampled by using the Monkhorst-Pack scheme with grid size 2x2x3 K points and the exchange-correlation function was GGA-PBESOL. The optimized rhodochrosite crystal structure was shown in Fig. 2. The optimized unit cell parameters are $a=b=4.8076 \text{ \AA}$, $c=15.6677 \text{ \AA}$, $\alpha=\beta=90^\circ$, $\gamma=120^\circ$. The unit

cell parameter error after crystal optimization is $\Delta a=0.64\%$, $\Delta c=0.02\%$, the error is within 1%, showing that the optimized crystal structure can be used for calculation.

The optimized rhodochrosite crystal structure was used to cleave the surface and build a vacuum layer. The thickness of the vacuum layer is 20 Å to construct the rhodochrosite (104) surface(Fig. 3(a)). In the structure of rhodochrosite (104) surface, one of the Mn atoms is replaced with Ca atom(Fig. 3(b)).

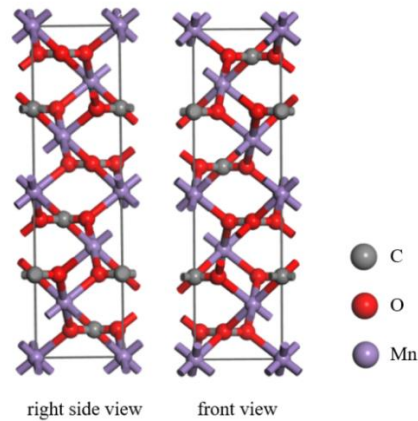


Fig. 1. The original crystals configuration of rhodochrosite

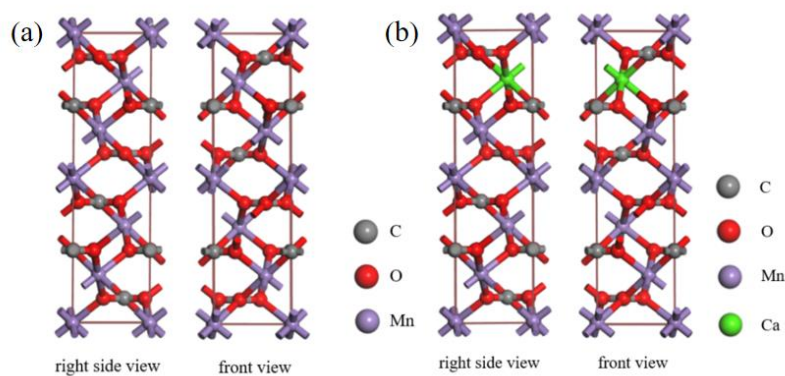


Fig. 2. The optimized crystal structure of rhodochrosite(a) and Ca substitution rhodochrosite(b)

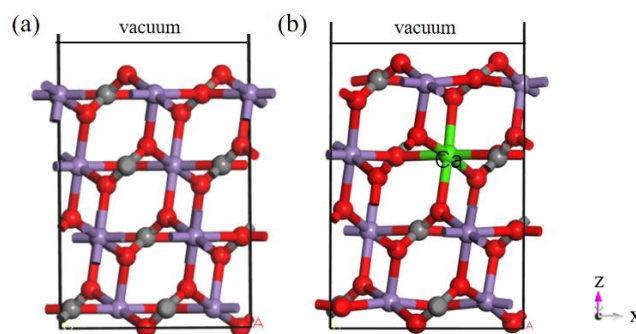


Fig. 3. Surface configuration of rhodochrosite (104)(a) and Ca substitution rhodochrosite (104)(b)

3. Results and discussion

3.1. Surface relaxation and reconstruction of rhodochrosite (104) surface

When rhodochrosite crystals form a cleaved surface, The arrangement of surface atoms is shown in Fig. 4(a), However, the broken chemical bond unbalances the normal force of the surface atomic chemical bond. The surface atoms are rearranged so that the interaction reaches a new equilibrium state (Wen, Deng et al., 2013).

According to the constructed rhodochrosite (104) surface, the O-Mn bond is broken on the rhodochrosite (104) surface. On the (104) surface of rhodochrosite, only Mn and O atoms have fracture structures, and C atoms do not form unsaturated bonds. Each Mn atom on the rhodochrosite (104) surface loses two O atoms, and its extranuclear negative charge decreases. Attracted by the negative charges of adjacent O atoms, Mn and O atoms approach each other (Wen, Deng et al., 2013). The relaxation and reconstruction of the first layer of atoms were shown in Table 1. By analyzing the relaxation and reconstruction, it can be found that the Mn and O atoms on the surface move toward the positive z-axis, and the displacement of O atoms is more obvious than that of Mn atoms. The lengths of C-O and O-Mn bonds on the surface before and after surface relaxation and reconstruction were shown in Table 2. After relaxation and reconstruction, the C-O bond formed by the O atoms close to the surface shortens, and the C-O bond formed by the O atoms away from the surface in the first layer elongates. The length of the O-Mn bond shortens after relaxation and reconstruction. The surface after relaxation and reconstruction is shown in Fig. 4(b).

It can be seen from Table 1 that the atoms in the first layer as a whole move along the negative direction of the x-axis and the positive direction of the z-axis. By comparing the moving distance of each atom in the z-axis direction, it can be found that the moving distance of C and O atoms in the z-axis direction is greater than that of Mn atoms. O23 and O4 atoms are in the outermost layer of the surface, and the moving distance to the positive z-axis is smaller than that of other O atoms. O18 and O8 atoms move the longest distance to the positive z-axis, and other O atoms move the distance to the positive z-axis less than the distance of C atoms. Through the study of rhodochrosite crystals, we found that the order of reactivity of atoms in rhodochrosite crystals is $Mn > O > C$. For the (104) surface, due to surface relaxation and reconstruction, the moving distance of C atoms in the positive z-axis direction is greater than that of Mn atoms and O atoms, while the moving distance of Mn atoms in the positive z-axis direction is smaller than that of O atoms. Therefore, C and O atoms with lower reactivity tend to be enriched on the (104) surface, while the Mn atoms with the highest reactivity tend to move away from the cleaved surface

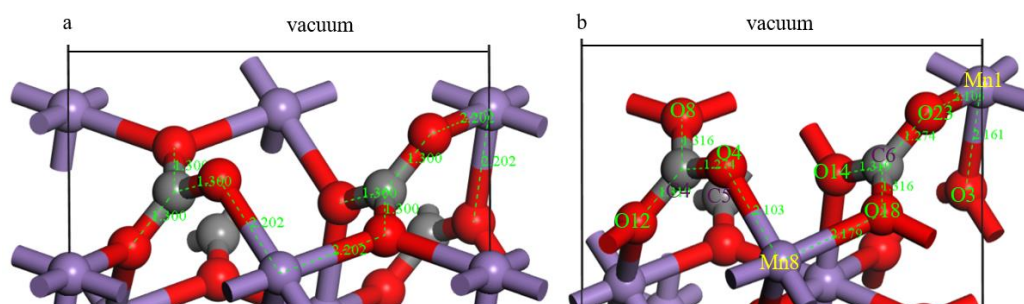


Fig. 4. Bond length comparison of C-O, O-Mn bond of not optimized(a) and optimized(b)

Table 1. Changes of atomic positions on the rhodochrosite (104) surface

	Number	Atomic displacement/Å		
		Δx	Δy	Δz
The first layer of Mn	Mn1	-0.0402	-0.0332	0.1988
	Mn8	-0.1086	0.0332	0.1973
	O8	-0.0306	-0.0435	0.4028
	O4	-0.0378	-0.0900	0.2988
The first layer of O	O23	-0.1063	0.0386	0.2973
	O18	-0.0990	-0.0079	0.4013
	O12	-0.0743	-0.0038	0.3224
	O14	-0.1427	-0.0476	0.3209
	C4	-0.0267	-0.0569	0.3557
The first layer of C	C6	-0.0951	0.0055	0.3542

Table 2. The lengths of C-O bond and O-Mn bond of the rhodochrosite (104) surface

Bond	bond length/Å	
	Before relaxation	After relaxation
C4-O4	1.300	1.274
C4-O8	1.300	1.316
C4-O12	1.300	1.319
C6-O14	1.300	1.319
C6-O18	1.300	1.316
C6-O23	1.300	1.274
Mn1-O3	2.202	2.161
Mn1-O23	2.202	2.103
Mn8-O4	2.202	2.103
Mn8-O18	2.202	2.179

3.2. The (104) surface electronic structure of rhodochrosite

3.2.1. Energy band of rhodochrosite

The properties of atoms on the constructed rhodochrosite (104) surface are different from those in the rhodochrosite crystal. Due to the breakage of the bonds between the surface atoms, the surface atoms are unsaturated and exhibit strong reactivity. According to the Energy Band Theory, due to the formation of the surface, the periodicity of the potential field is destroyed. The periodicity of the potential field in Bloch's theorem is discontinuous, which causes the electron energy levels of surface atoms to enter the band gap and form a new surface state energy level.

The band gap is one of the important characteristic parameters of semiconductors. Band gap value is related to the energy band structure. A large number of electrons in the valence band are valence electrons, and the reactivity of surface atoms can be judged by analyzing the activity degree of electrons in the band structure (Koster et al., 1981). During the flotation process, when the electrochemical reaction and adsorption occur on the mineral surface, the higher the electron state density of the atom near the Fermi level, the stronger the reactivity of the atom (Chen 2015).

Fig. 5 shows the energy band diagram of rhodochrosite crystal and the rhodochrosite (104) surface. Compared with the energy band diagram of rhodochrosite crystal, the following conclusions can be drawn. The energy band on the surface of rhodochrosite is denser than the crystal. This is because the surface model has more atoms than the crystal. The band gap width on the rhodochrosite surface is reduced to 1.614 eV. This change in the band gap width shows that the formation of the surface has caused a significant change in the electronic structure. The valence band on the rhodochrosite (104) surface is closer to the Fermi level than the rhodochrosite crystal, so the electrons on the rhodochrosite (104) surface are more active than the electrons of rhodochrosite crystal.

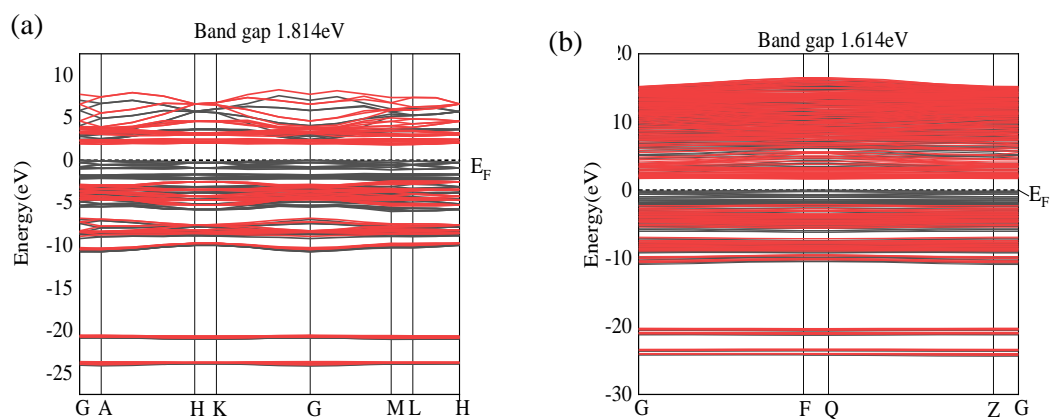


Fig. 5. The energy band diagram of the crystal (a) and (104) surface of rhodochrosite

The energy band line of the conduction band on the surface of rhodochrosite is flatter than the rhodochrosite crystal, indicating that the effective mass of electrons at the bottom of the conduction band on the rhodochrosite (104) surface has increased and the localization of electrons has become stronger. The valence bands on the rhodochrosite (104) surface and crystal have reached the Fermi level, indicating that the rhodochrosite has a certain degree of metallicity, and the electrons are easy to transition to the conduction band. Therefore, after the (104) surface is formed, the electrical conductivity and electrochemical activity are improved compared to rhodochrosite crystals.

3.2.2. Energy band of surface and crystal after Ca substitution

Compared to the energy band diagrams of the rhodochrosite crystal and (104) surface after the Ca substitution. The band gap width of the rhodochrosite (104) surface after the Ca substitution decreased from 1.906 eV to 1.654 eV. It shows that the electronic structure of the surface and crystal of the rhodochrosite after Ca substitution is obviously different. Increased energy required for electronic transitions. The band line of the conduction band on the rhodochrosite surface after the Ca substitution is flatter than the crystal. It shows that the effective mass of electrons at the bottom of conduction band on rhodochrosite the (104) surface after Ca substitution increases, and the localization of electrons becomes stronger. Compared with the rhodochrosite crystal after the Ca substitution, the electron energy band moves to a lower energy level as a whole, and the Fermi level passes through the conduction band. This shows that the atoms on the rhodochrosite (104) surface after the substitution of Ca atoms are more stable than those on the rhodochrosite crystal after the substitution of Ca atoms.

3.2.3. Effect of Ca atom substitution on the surface energy band structure of rhodochrosite (104)

According to Fig. 5 and Fig. 6, compared with the changes of the rhodochrosite surface before the substitution, the band gap width of the rhodochrosite after the substitution is greater, indicating that the (104) surface formed after Ca substitution requires more energy for electrons to transition from the valence band to the conduction band. The (104) surface atom electrochemical activity after Ca substitution is more stable than that of unsubstituted surface atoms. The surface energy band diagram after Ca substitution moves to a lower energy level. Due to the existence of impurity atoms, the electron energy band moves to a lower energy level as a whole, Fermi level passes through the conduction band. Through comparing and analyzing Fig. 5(b) and Fig. 6(b), find that the Ca substitution makes the band gap of the rhodochrosite (104) surface widen, so the Ca substitution reduces the electrical conductivity and electrochemical activity of the rhodochrosite (104) surface.

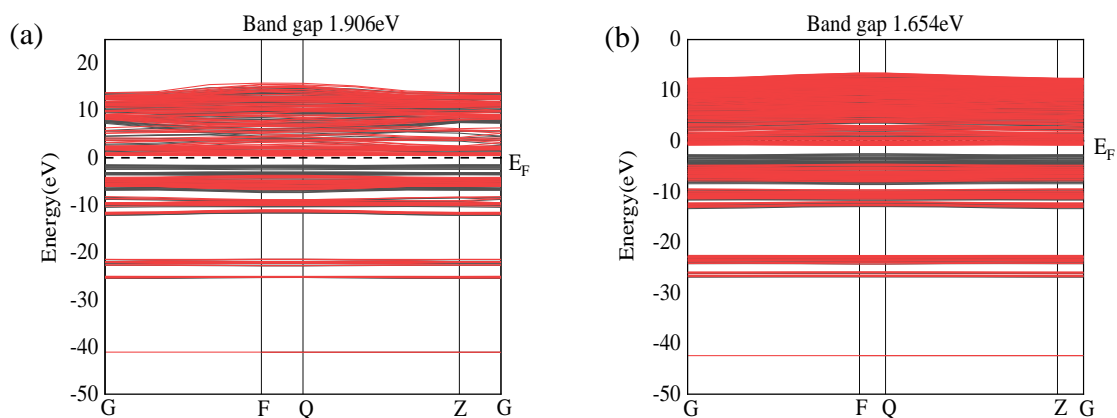


Fig. 6. Energy band diagram of crystal and rhodochrosite (104) surface after Ca substitution

3.2.4. The density of states of rhodochrosite before and after Ca substitution

Compared to the density of states map of the rhodochrosite (104) surface and crystal, it can be seen that the density of states peaks of the surface orbitals near the Fermi level are higher than that of the crystal orbitals, indicating that the reactivity of atoms increases after the (104) surface is formed. The

contribution of the p orbital near the Fermi level in the crystal is less than that of the p orbital farther from the Fermi level. After the surface is formed, the contribution of the p orbital near the Fermi level is greater than that of the p orbital farther from the Fermi level. The two p-orbital density peaks below the Fermi level are mainly contributed by O atoms, indicating that the reactivity of O atoms is enhanced after the surface is formed. In the same way, it can be seen that after the surface is formed, the reactivity of Mn atoms also increases.

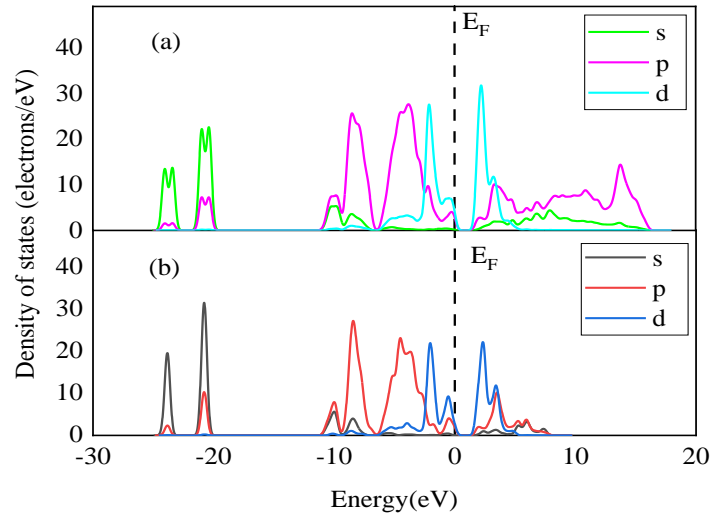


Fig. 7. The density of states of the (104) surface (a) crystal of rhodochrosite(b)

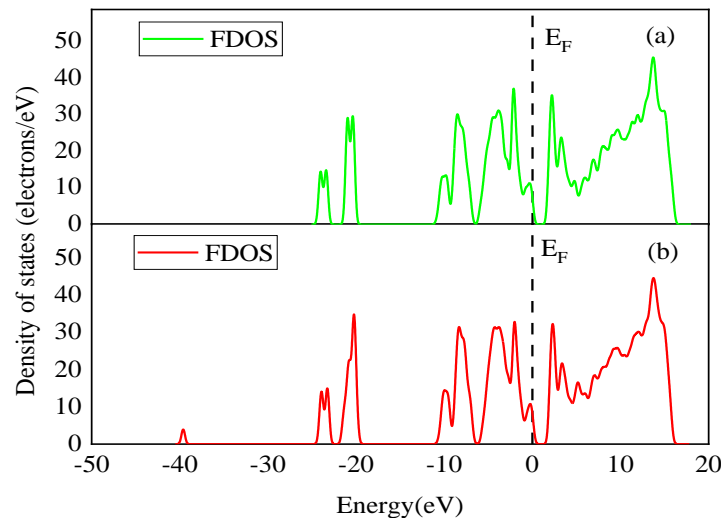


Fig. 8. FDOS of (104) surface of rhodochrosite (a) and rhodochrosite (104) surface after Ca substitution (b)

It can be seen from Fig. 8 that the FDOS peak near the Fermi level on the rhodochrosite (104) surface after Ca substitution decreases, indicating that the reactivity of atoms on the rhodochrosite surface decreases after the Ca substitution.

3.3 Influence of Ca atom substitution on the surface electrical properties of rhodochrosite

By analyzing the energy band diagram of unsubstituted rhodochrosite, it is concluded that rhodochrosite has a certain degree of metallicity, a small band gap, and certain semiconductor characteristics. Electrons tend to move away from the surface. This is confirmed by the analysis of surface atomic charges. The charge on the unsubstituted rhodochrosite surface is $0.64e$, and the charge on the bulk layer is $0.12e$. It shows that the bulk layer is in an electron-rich state and the surface layer is in an electron-deficient state. Electrons in the surface layer flow from the surface to the bulk phase, causing the loss of electrons in the surface layer. Therefore, it can be considered that the positive

charge of the surface layer is enriched, so the surface of rhodochrosite has the characteristic of absorbing external electrons. This is one of the reasons for the use of anionic collectors in the flotation process.

The rhodochrosite surface has positive charge enrichment, and the surface has the characteristic of absorbing external electrons. The charge on the surface layer of the rhodochrosite after Ca substitution is $0.59e$, and the charge on the bulk layer is $0.05e$. Compared with the charge on the surface layer and bulk layer of unsubstituted rhodochrosite, the charge on the surface layer is decreased. It shows that after the substitution of Ca, the charge on the surface of the rhodochrosite decreases, the absorption capacity of external electrons decreases, and the surface electrical properties decrease.

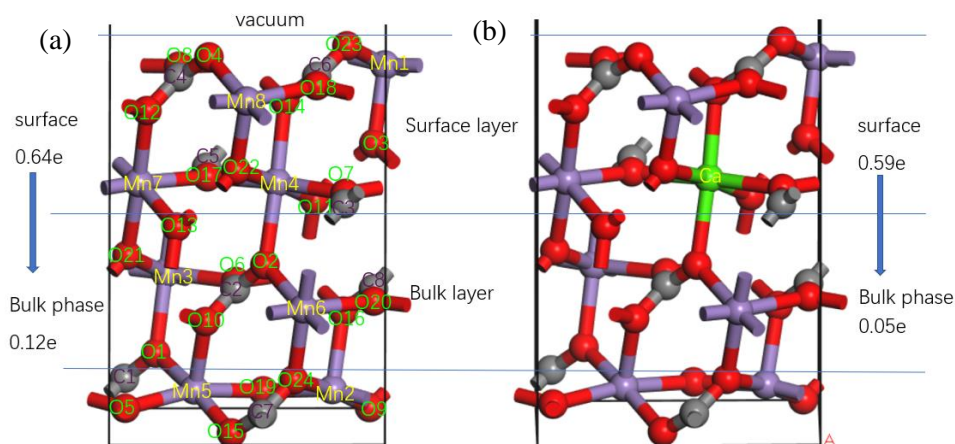


Fig. 9. Surface atom numbering and layering of rhodochrosite before (a) and after (b) Ca substitution (a is the structure before replacing, b is the structure after replacing)

4. Conclusions

After rhodochrosite formed (104) surface, the C and O atoms with low reactivity tend to enrich on the surface, while the Mn atoms with the highest reactivity tend to be away from the surface, which leads to the decrease of the reactivity on the surface of rhodochrosite.

The atoms on the rhodochrosite (104) surface substituted by Ca are more stable than those on the unsubstituted rhodochrosite (104) surface. After Ca substitution, the electron gain characteristic of O atom increases, while the electron loss characteristic of metallic element and C atom decreases. Therefore, after the rhodochrosite crystals form the (104) surface, the oxidizability decreases and the reducibility increases. the Ca substitution reduces the electrical conductivity and electrochemical activity of the rhodochrosite (104) surface.

The rhodochrosite (104) surface has positive charge enrichment, and the surface has the characteristic of absorbing external electrons. After the substitution of Ca, the charge on the surface of the rhodochrosite decreases, the absorption capacity of external electrons decreases, and the surface electrical properties decrease.

Acknowledgments

The authors gratefully acknowledge the financial support of National Key R&D Program of China (No.2018YFC1903500).

References

- BENTARCURT, Y.L., CALATAYUD, M., KLAPP, J., et al., 2018. *Periodic density functional theory study of maghemite (001) surface. Structure and electronic properties.* Surface Science 677.
- CHEN, J. 2015. *The solide physics of sulphide minerals flotation:* Central South University Press: Changsha, China.
- CHEN, J., XU, Z., CHEN. Y., 2020. *Electronic structure and surfaces of sulfide minerals: Density functional theory and applications:* Elsevier.

- CHEN, J.H., CHEN, Y., YU-QIONG, L.I., 2010. *Quantum-mechanical study of effect of lattice defects on surface properties and copper activation of sphalerite surface*. Transactions of Nonferrous Metals Society of China 20 (006), 1121-1130.
- GRAF, D.L. 1961. *Crystallographic tables for the rhombohedral carbonates*.
- HE, G., LI, K., LI, S., GUO, T., HUANG, C., ZENG, Q., 2020. *First-principles calculations of electronic structure of rhodochrosite with impurity*. Physicochemical Problems of Mineral Processing 56.
- KIRCHMEYER, S., REUTER, K., 2005. *Scientific importance, properties and growing applications of poly(3,4-ethylenedioxythiophene)*. J.mater.chem 15 (21), 2077-2088.
- KOSTER, F. G. 1981. *Solid state physics*. Science 211 (4479):272-272.
- LUO, N., WEI, D.Z., SHEN, Y.B., LIU, W.G., GAO, S.L., 2018. *Effect of calcium ion on the separation of rhodochrosite and calcite*. Journal of Materials Research and Technology 7 (1), 96-101.
- MILMAN, V., REFSO, K., CLARK, S.J., PICKARD, C.J., 2010. *Electron and vibrational spectroscopies using dft, plane waves and pseudopotentials: Castep implementation*. Journal of Molecular Structure: THEOCHEM 954 (1-3), 22-35.
- MONKHORST, H.J., PACK, J.D., 1976. *Special points for brillouin-zone integrations*. Physical review. B, Condensed matter 13 (12), 5188-5192.
- MORAWSKI, I., KUCHARCZYK, R., NOWICKI, M., 2016. *Surface relaxation of pt(1 1 1) and cu/pt(1 1 1) revealed by depes*. Applied Surface Science.
- OLIVEIRA, C.D., DUARTE, H.A., 2010. *Disulphide and metal sulphide formation on the reconstructed (0 0 1) surface of chalcopyrite: A dft study*. Applied Surface Science 257 (4), 1319-1324.
- PARKER, J.S., DOHERTY B., TAYLOR, K.T., SCHULTZ, K.D., BLAGA, C.I., DIMAURO, L.F., 2006. *High-energy cutoff in the spectrum of strong-field nonsequential double ionization*. Physical Review Letters 96 (13), 133001.
- PFROMMER, B.G., COTE, M., LOUIE, S.G., COHEN, M.L., 1997. *Relaxation of crystals with the quasi-newton method*. Journal of Computational Physics 131 (1), 233-240.
- RAHIMI, S., M. IRANNAJAD, MEHDILO., A., 2017. *Comparative studies of two cationic collectors in the flotation of pyrolusite and calcite*. International Journal of Mineral Processing 167, 103-112.
- SARVARAMINI, A., LARACHI, F., 2017. *Understanding the interactions of thiophosphorus collectors with chalcopyrite through dft simulation*. Computational Materials Science 132, 137-145.
- VANDERBILT, DAVID. 1990. *Soft self-consistent pseudopotentials in a generalized eigenvalue formalism*. Physical Review B Condensed Matter 41 (11), 7892.
- WEN, S.M., DENG, J.S., XIAN, Y.J., DAN, L., 2013. *Theory analysis and vestigial information of surface relaxation of natural chalcopyrite mineral crystal*. Transactions of Nonferrous Metals Society of China 23 (3), 796-803.
- YANAI, T., TEW, D.P. HANDY, N.C., 2004. *A new hybrid exchange-correlation functional using the coulomb-attenuating method (cam-b3lyp)*. Chemical Physics Letters 393 (1-3), :51-57.
- ZHANG, W., CHENG, C.Y., 2007. *Manganese metallurgy review. Part i: Leaching of ores/secondary materials and recovery of electrolytic/chemical manganese dioxide*. Hydrometallurgy 89 (3-4), 137-159.
- ZHOU, F., YAN, C., WANG, H., SUN, Q., WANG, Q., ALSHAMERI, A., 2015. *Flotation behavior of four c18 hydroxamic acids as collectors of rhodochrosite*. Minerals Engineering 78, 15-20.
- ZHU, G., CAO, Y. WANG, Y., WANG, X., MILLER, J.D., LU, D., ZHENG, X., 2020. *Surface chemistry features of spodumene with isomorphous substitution*. Minerals Engineering 146, 106139.